RESEARCH AND DEVELOPMENT OF POWER DETECTION TECHNOLOGY AND DEVICE FOR KEY PARTS OF GREEN FODDER HARVESTER
/
基于青饲收割机关键部件的动力检测技术与设备的研究与开发

Kang NIU[1,2)], Xiaoyi CUI[1,2)], Ruikang QIN [1,2)], Yuqi WANG[1,2)], Weijing WANG[1,2)], Liming ZHOU[1,2)], Yangchun LIU[1,2)], Fengzhu WANG[1,2)], Dongyang WANG[3)], Weipeng ZHANG[1,2*)]
[1)]Chinese Academy of Agriculture Mechanization Sciences Group Co., Ltd, Beijing 100083
[2)]State Key Laboratory of Agricultural Equipment Technology, Beijing 100083
[3)]Shenzhen Polytechnic University, Shenzhen, Guangdong, China 518055
Corresponding author: Weipeng Zhang
DOI: https://doi.org/10.35633/inmateh-74-05

Keywords: *corn forage harvester, sensor design, power detection, CAN-bus, test analysis*

ABSTRACT
The study focuses on the self-propelled forage harvester and analyzes various parameters such as the working speed and torque of the cutting table, chopped roll, throwing fan, walking parts, and the output flow rate and pressure of the hydraulic pump of the feeding section. Field experiments show that the fan, walking, chopping roller, and grain crushing roller drive powers account for 7-8%, 7-10%, 24-28%, and 13-21% of the engine power, respectively. The driving power of the inner and outer sides of the cutting table, fan, and walking power account for a relatively stable proportion of the engine output power. The study collects and analyzes operation parameters simultaneously to provide a reference for evaluating the performance and optimizing the design of corn forage harvesters.

摘要
本研究针对自走式饲草收割机进行深入探讨，系统分析了切割台、碎料辊、抛送风扇、行走机构等关键部件的工作速度与扭矩特性，以及送料部分液压泵的输出流量与压力等重要参数。通过实地试验，研究发现风扇、行走机构、切碎滚筒和谷物破碎滚筒的驱动功率分别占发动机总功率的 7-8%、7-10%、24-28%和 13-21%，且切割台内外侧、风扇及行走功率分配相对稳定。本研究同步收集并分析了运行参数，旨在为玉米饲草收割机的性能评估及设计优化提供科学依据。

INTRODUCTION
China is a large agricultural country with about 1.8 billion mu of arable land. There are many kinds of crops, such as rice, wheat, corn, green fodder, and so on. The popular use of combine harvester mechanization level is increasing, automation, intelligence and standardization have become the trend in agricultural machinery development (*Mao et. al., 2020*). Currently, there are functions for monitoring, displaying, and alerting the rotational speeds of key rotating components in small and medium-sized combine harvesters, such as fans, threshing cylinder engines, and other essential parts. (*Liang et. al., 2023*). However, due to the relatively independent relationship between the parameters, it is impossible to control the association, and it is difficult to realize the automatic adjustment of the working parameters during the harvesting process to achieve the best harvesting quality of the operating state (*Wang et. al., 2023*).

Scholars at home and abroad have carried out a lot of research work on combine harvester operation power monitoring (*Mohsenimanesh et. al., 2017, Siebald et. al., 2017*), mainly using torque and speed to realize power online monitoring. Foreign green fodder harvesting machinery has been completely developed in the direction of automation, informatization, and intelligence. The representative results include, for example, the Case IN 8010 model developed by Case which is equipped with a power optimization system, power acquisition system, and operation quality monitoring system. During field harvesting, the collected loss rate and power are used as the control target of the power optimization system, which greatly improves the operation quality of the combine harvester (*Pallottino et. al., 2019, Feuerstein et. al., 2014*), which greatly improved the overall performance and automation level of the whole machine. *Cho et. al., (2014)*, proposed a method to detect uncut crop edges during harvester operation using multiple sensors, which provided more valuable information for combine harvester operation monitoring.

Cho et. al., (2021), proposed a method to accurately capture field spatial variability of corn forage and corn grain yield in the New York method that generated the most accurate grid maps of corn forage and grain yields at both the farm and field levels. It is useful to ensure accurate and precise spatial mapping of yield products to optimize corn growth management.

With modern agriculture showing intensive and large-scale development, high-end large-scale agricultural machinery and equipment play an increasing role in China's agricultural production, therefore, there is an urgent need for the corresponding field experiment validation methods and key parts and components of the operational parameters acquisition technology. The corresponding collection test devices and systems are developed (*Wang, 2019*). The field operation quality and operation load monitoring technology of the combine harvester were studied, and the acquisition system of threshing roller load characteristics was designed. The current research mainly detects single or several machine parameters, and the detection data are relatively independent of each other, lacking systematic basic data on operation quality and component working conditions, and the method of correlation analysis (*Chen, et. al., 2023, Zhou, et. al., 2023*). *Liu et. al., (2022),* proposed a new semantic segmentation network RSHC U-Net for self-propelled forage harvesters to achieve better trailer hopper segmentation in forage harvesting images. Experts and scholars carried out corresponding control research on key parts of the combine harvester such as the fan, threshing roller, etc., and controlled them independently, collected the corresponding operating state parameters, and formulated the standards of precise control system (*Zhang et. al., 2022, Li et. al., 2021, Wu et. al., 2024*), breaking through the combine harvester intelligent working condition monitoring technology and intelligent control technology (*Martelli et. al., 2015, Liu et. al., 2022*). *Buryanov et. al., (2019),* developed a method for stripping plants from their roots, and this method has been proven to enhance the productivity and efficiency of combine harvesters by a factor of 1.4 to 2.0. *Zhou et. al., (2020),* developed an effective step-less speed regulation mechanism for real-time control of the threshing drum and cleaning fan in combine harvesters.

This study is oriented to the field operation of corn forage harvester, to solve the key problems of insufficient field experiment data and lack of test validation means of China's agricultural machinery and equipment, focusing on research on field operation of the whole machine and the core working device power matching detection method, to provide testing technology support for the rapid acquisition of operational data of the test validation and performance evaluation system.

MATERIALS AND METHODS

Power monitoring methods

The cutting table, threshing roller, cleaning sieve, chopping roller and blowing fan are the core working parts of the forage harvester, and their working power is one of the key information for determining the working status and fault condition of the machinery in the field if the working load of the parts is too large, it is easy to lead to clogging of the rotating shaft, which will cause a serious impact on the driving parts; if the load is too small, the parts are in the unsaturated working state, and the feeding amount is insufficient, which affects the harvesting efficiency. In the harvesting process of corn forage harvester, the power of these core working mechanisms should be ensured to be in a better state as far as possible, so it is necessary to carry out on-line dynamic monitoring of the working power of the key working parts, to provide basic data support for the reasonable power distribution of the key working parts as well as the analysis of the influence of the working power of each part on the quality of the machine operation.

The most direct and effective way to monitor the power of the working parts is the online monitoring of the torque and speed of the rotating working shaft, as shown in Figure 1.

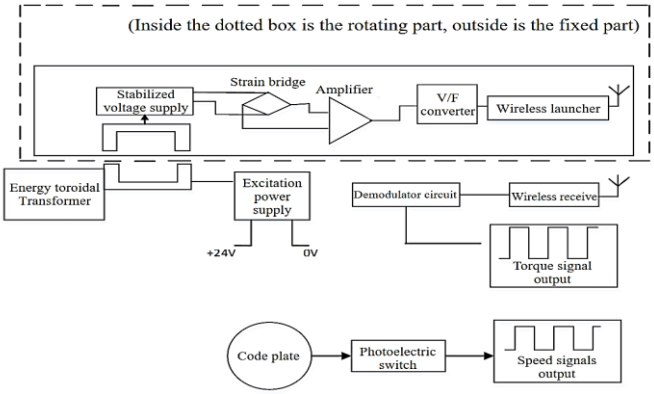

Fig. 1 - The principal diagram of the torque sensor

In this study, a specially designed and customized rotary strain-type torque sensor is used, applying the strain bridge electrical measurement technology, the special torsion-measuring strain gauges are pasted on the measured elastic shaft with strain adhesive to form a strain bridge, and a set of toroidal transformers located on the sensor provide power supply to the strain bridge non-contact, and amplify the weak elastic shaft subjected to torsion signals detected by the strain bridge, convert the voltage/frequency (V/F), so as to make the torque value be proportional to the measured frequency value, and finally a micro-power signal coupler is used to replace the toroidal transformer for non-contact transmission to output its frequency signal, which can effectively overcome the high-order harmonic generation brought about by the inductive coupling and the mutual interference between the energy toroidal transformer and the signal toroidal transformer, and its internal rotational speed measurement device based on the Hall element is also included.

The torque sensor uses a toroidal transformer non-contact transfer of energy, signal output using wireless telemetry, the torque signal wireless transmission is converted to wired transmission, thereby overcoming a series of problems such as torque angle phase difference, strain bridge collector ring issues, battery power supply concerns, and radio telemetry limitations.

Power monitoring principle

Conventional torque speed sensors require the use of a broken shaft to connect the sensor in series between the power source and the load, as shown in Figure 2. This kind of mounting form will cause great inconvenience to the sensor installation. For this reason, several new structures of torque speed sensors are designed in this study: strain gauges on the shaft method, extended shaft method, and replacement pulley method. Among them, the extended shaft method changes the transmission route of the original power, through the modification of the mechanical structure of the pulley, disconnecting the power transmission between the pulley and the pulley of the load shaft, the pulley first drives the inner rotary shaft of the torque-speed monitoring sensor, and then the outer rotary shaft of the torque-speed monitoring sensor transmits the power back to the load shaft, and the load condition of the working shaft can be obtained by the strain-bridge circuit affixed in the inner and outer shafts of the torque sensor. The load condition at the working shaft can be obtained through the strain bridge circuit attached between the inner and outer shafts of the torque sensor. The extended shaft method fixes the pulley disk of the torque sensor to the outer side of the rotating shaft through a number of bolts, and the head of the rotating shaft needs to be embedded in the rotating sleeve of the sensor, which in effect installs the sensor with a torque signal coupler between the power source and the load without disconnecting the drive shaft. The replacement pulley method is the application of the elastic modulus coefficient of better materials to make the power wheel, replace the original pulley, the use torsion strain gauges to detect the elasticity of the power wheel elastic deformation, so as to indirectly obtain the torque at the working shaft, and without the need to disconnect the shaft to complete the torque monitoring of the components.

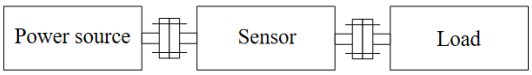

Fig. 2 - The connection diagram of the torque sensor

Corn forage harvester machine power detection technology

Torque Sensor Design

(1) Design of torque sensors for forage harvesters

The torque and speed monitoring sensor structure of each component of the forage harvester is designed by adopting various torque sensors such as the shaft-mounted type, the replacement pulley type, the hydraulic pressure and flow type, etc., as shown in Figure 3, including the walking parts, working hydraulic pump, cutting table large blade, cutting table small blade, chopping roller, clearing fan and grain crushing roller and other seven key working parts.

(a) Walking spline shaft **(b) Chopping roller** **(c) Cutting table large and small size blade**

(d) Clearing fan (e) Grain crushing rollers

Fig. 3 - The torque and speed monitoring sensor of the forage harvester

Among them, some of the sensor prototypes of the two types of sensors for corn harvesting are shown in the physical drawings as in Figure 4. The designed torque monitoring sensor outputs a frequency pulse signal of 10 kHz at no load, 15 kHz at full load for forward rotation, and 5 kHz at full load for reverse rotation, with a full-scale measurement accuracy of 0.5%. In addition, a rotational speed sensor is integrated into the torque measuring device, and the working power of the rotating parts can be deduced according to:

$$P = T \times n / 9549 \quad [kW]$$

In the aforementioned equation, *P* denotes power, [kW], *T* signifies torque, [N m], and *n* represents the rotational speed of the motor, [r/min].

According to the driving power of the corn forage harvester, the working torque of the rotating parts at all levels is estimated, to determine the range of the torque sensor as 0 to 1500 Nm and 0 to 1000 Nm two kinds.

Fig. 4 - The prototype of the torque and speed monitoring sensor

Torque sensor calibration

The use of JZ200 torque sensor static calibration table on the selected torque sensor for static calibration, is shown in Figure 5.

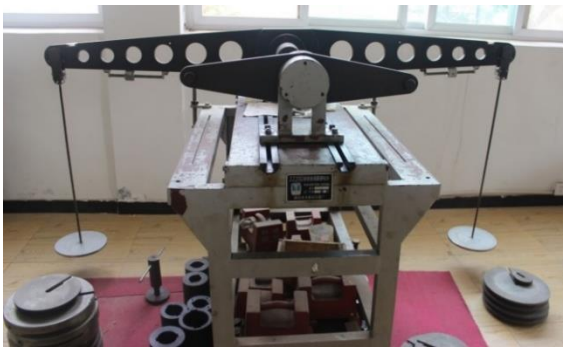

Fig. 5 - The JZ200 static calibration device of the torque sensor

According to the formula $T = F' \cdot S$, where F' is the force perpendicular to the cross-section axis of the torque sensor, and S is the distance from force F' to the cross-section axis of the torque sensor. The torque sensor is calibrated to carry out the accuracy test of torque measurement, respectively, to the static calibration table loaded with different masses of standard weights, the system measurement value is recorded, then analyzing and processing is performed and the torque sensor's measurement error is obtained within 0.5%.

Among them, the torque sensor of the engine output intermediate shaft has a range of 1500 Nm and an operating voltage of 24 V. The static calibration was carried out in a room with a temperature of 22°C and a humidity of 60 % to obtain an accuracy of 0.5 % F.S. as shown in Table 1.

Table 1

The calibration results of the torque sensor in the engine output shaft

Load value [Nm]	Positive Signal Frequency output (kHz)		Reverse Signal Frequency output (kHz)	
	load	uninstallation	load	uninstallation
0	10.005	10.005	10.005	10.005
300	11.011	11.012	9.000	9.000
600	12.017	12.017	7.994	7.995
900	13.023	13.023	6.989	6.990
1200	14.029	14.029	5.983	5.985
1500	15.035	15.035	4.980	4.980

The range of the clearing fan shaft torque sensor is 1000 Nm, the operating voltage is 24 V, and the static calibration is carried out at a room temperature of 22°C and a humidity of 60% to obtain an accuracy of ±0.5 % F.S, as shown in Table 2.

Table 2

The calibration results of the torque sensor in clearing the fan shaft

Load value [Nm]	Positive Signal Frequency output (kHz)		Reverse Signal Frequency output (kHz)	
	load	uninstallation	load	uninstallation
0	10.005	10.005	10.005	10.005
200	11.010	11.009	9.002	9.003
400	12.015	12.015	8.000	8.000
600	13.020	13.020	6.997	6.998
800	14.025	14.025	5.995	5.995
1000	15.030	15.030	4.993	4.993

To test the dynamic performance of torque measurement, the procedure involves first controlling the speed of the test shaft to reach the preset desired value and maintaining stable operation for a certain period of time. After that, the test shaft is stopped and returned to its initial working state. Once the test shaft has completely stopped, the entire measuring system is shut down. The resulting dynamic step response curve of the torque sensor is illustrated in Figure 6.

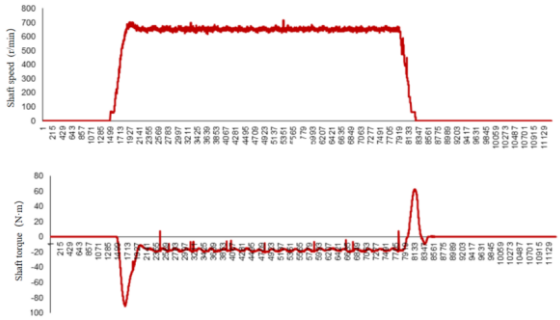

Fig. 6 - The dynamic loading curve of the torque sensor

As can be seen from the figure, the torque of the measured shaft is consistent with the trend of the rotational speed change. When the rotational speed of the measured shaft does not change, the torque measurement value basically remains stable, and when the rotational speed of the measured shaft suddenly increases or decreases, the torque measurement value enters a new steady state after a large transient pulse, which is in line with the torque change rule under the normal working condition of rotary shafts, indicating that the torque sensor designed in this research has good performance, and is able to monitor the torque information of the above key working shafts effectively. It shows that the torque sensor designed by this institute works well and can effectively monitor the torque information at the above key working shaft.

Vehicle-mounted data communication network

All the data from the vehicle-mounted sensors are sent to the host computer through the CAN-bus network for display and saving, as Figure 7 shows. The CAN network supports up to 110 nodes, simplifying circuit connections via a bus architecture for easy installation. Nodes communicate freely using differential signaling, often through shielded twisted-pair cables for robust anti-jamming. Additionally, it offers considerable communication distance.

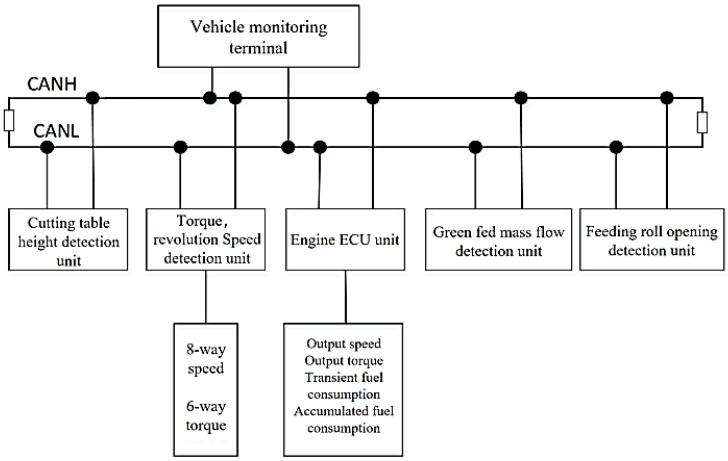

Fig. 7 - The network structure of CAN-bus communication in forage harvester

Each detection unit is a CAN node composed of a sensor, an acquisition controller and a CAN communication module. The acquisition controller collects data from on-site sensors in real time and saves the processing results in a memory unit, and it also has a network-wide unique identifier (ID) bound to a specific sensor. The vehicle monitoring terminal periodically sends out remote data query frames in accordance with the CAN2.0B protocol using the USB-CAN adapter. When the collection controller receives the remote frames, it compares its own ID with the ID of the remote frames, and if it matches, it returns a data frame containing the sensor data using its own ID as the identifier, and sends it to the bus network through the CAN communication module, and the monitoring computer, after receiving the data frames, updates the corresponding sensors according to their IDs. When the monitoring computer receives the data frame, it updates the data of the corresponding sensor according to the ID, thus realizing the real-time display and saving of the signals of each torque and speed sensor.

Power Acquisition Controller

The power monitoring system mainly involves the pulse signal acquisition of relevant torque sensors and speed sensors. Therefore, this study adopts PIC18F2580 as the processor for the design of the power acquisition controller and configures various peripheral hardware circuits with PIC18F2580 as the core to constitute a complete power monitoring controller hardware. The system structure is mainly composed of a microcontroller minimum system, pulse input signal acquisition and CAN data communication and other subsystems.

The CAN communication protocol in this study follows the SAE J1939 standard. It is a network protocol for high-speed communication between multiple ECUs that supports closed-loop control and has become a common standard for controller local area networks in trucks and buses. It uses CAN 2.0 as the core of the network, and each node in the network has a network-wide unique 29-bit J1939 identifier that identifies the type of parameter being transmitted on the CAN-bus network.

The pulse signals are counted by the 16-bit counters Timer0 and Timer1 within the microprocessor PIC18F2580, and the 16-bit timer Timer3 is used for timing, and the timing time selected in this study is 0.1 s. The timer block diagram is shown in Figure 8.

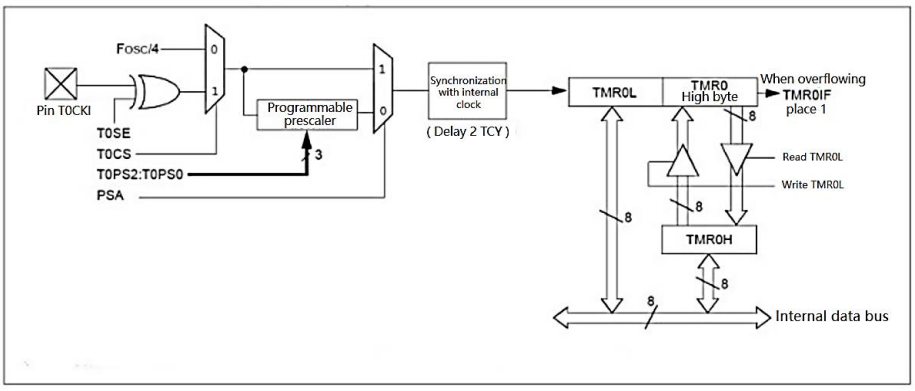

Fig. 8 - The timer block diagram

Its internal software acquisition process, is shown in Figure 9.

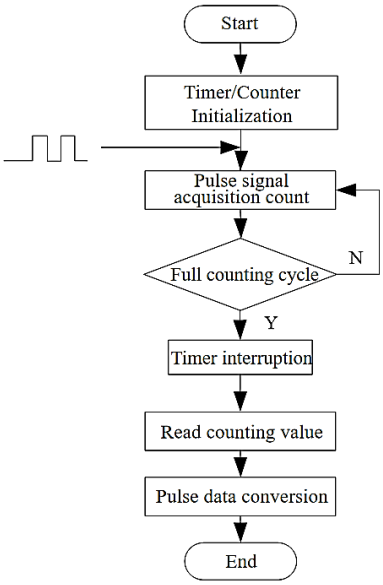

Fig. 9 - The program flow chart of pulse sampling

The PIC18F2580 microcontroller selected for this study incorporates the communication controller ECAN module, which follows the Bosch specified CAN2.0A or CAN2.0B protocol. The CAN-bus module consists of a protocol engine with a message buffer and a control module. The CAN protocol engine automatically handles all the functions of receiving and sending messages on the CAN-bus. Messages are sent by first loading the corresponding data registers. Status and errors can be detected by reading the corresponding registers. Any message detected on the CAN-bus is detected for errors and subsequently compared with a filter to determine whether it should be received and stored in one of the two receive registers. The internal software design consists of 3 main parts: initialization of the CAN node, data transmission and data reception.

Initialization is a crucial part of the CAN communication system's operation, serving as the prerequisite for the normal functioning of the CAN-bus. Initialization design includes the configuration of CAN module working mode, interrupt allow register setting, baud rate parameter setting, receive shield register setting, transmit priority setting and receive filter setting, etc., as shown in Figure 10.

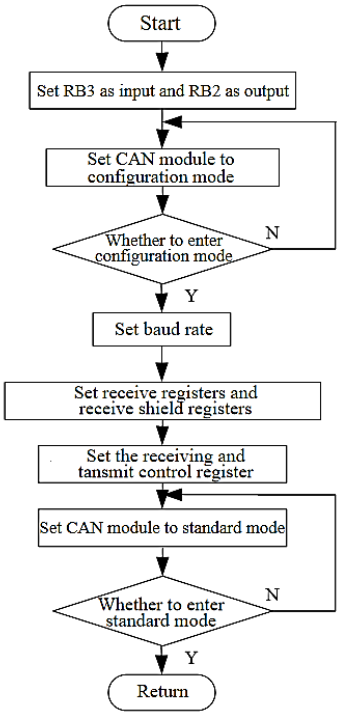

Fig. 10 - The flow chart of CAN initialization in the data acquisition controller

Selection of test factors

The travel speed of the self-propelled forage harvester is an important factor affecting the power consumption, and the change in travel speed will cause the change in feeding volume, with the increase in feeding volume, the rotational speed of each key part decreases slightly, and the torque rises, and the power consumption of the self-propelled forage harvester roughly shows an upward trend. At the same time, the height of the cutting table also affects the power consumption; at the same travel speed, the lower the height of the cutting table, the smaller the stubble height, and the feeding volume increases at the same time, in the process of the test. The local farmers in order to obtain a higher yield often require drivers to reduce the height of the cutting table to a minimum, generally 200 mm. In summary, the travel speed and height of the cutting table were selected as the two factors for the test arrangements. The machine's travel speed during normal operation is within the range of 3-10 km/h, and the height of the cutting table during normal operation is within the range of 150 mm to 250 mm, and the test arrangement is shown in Table 3.

Table 3

Operational test schedule

Test	1	2	3	4
Travel speed (km/h)	3	5	7	10
Cutting table height (mm)	200	200	200	200

Experimental Methodology Design

The field with good silage corn growth, length, and width meeting the test requirements was selected as the test area, and the corn at the starting point was harvested with the prototype before the test started to ensure the smooth start of the prototype. The operation of the self-propelled forage harvester and the acquisition of relevant data were carried out in accordance with the national standard GB80097-2008 “Test Methods for Harvesting Machinery Combine Harvester”. Before entering the measurement area, the travel speed of the self-propelled forage harvester and the rotational speed of each key part reached a predetermined value and stabilized, and then entered the measurement area at a constant speed to start measurement. Each test was harvested in full width (cutting width 6 m), and the length of the harvesting interval and operating time were recorded during the test, and each group of tests was repeated twice to take the average value, and the condition of the machine was checked at the end of each group of tests, so as to be carried out in the next test. The condition of the prototype machine in the field test is shown in Figure 11.

Fig. 11 - Test prototype field operation

RESULTS

The system is capable of capturing real-time torque and rotational speed data for various critical components of the self-propelled forage harvester throughout its entire journey from entering the test area to exiting. Subsequently, it accurately calculates the power consumption of these critical components based on different test conditions. Figure 12 presents a clear illustration of the working power consumption curves for some experimental groups of the self-propelled forage harvester, with all these data derived from the aforementioned real-time data acquisition and calculation process. The power curves in the figure, from top to bottom, represent the chopping roller driving power, fan driving power, grain crushing roller driving power, walking driving power, outer cutting table driving power, and inner cutting table driving power.

To visualize the above contents more concretely and reflect the load fluctuation of the operating components, the average power and standard deviation under the four test conditions were calculated as shown in Table 4 and Table 5.

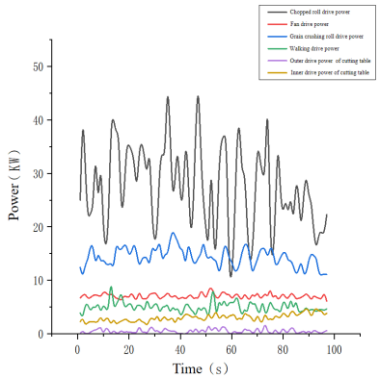

a) Average speed of 2.21 km/h, stubble height of 200 mm

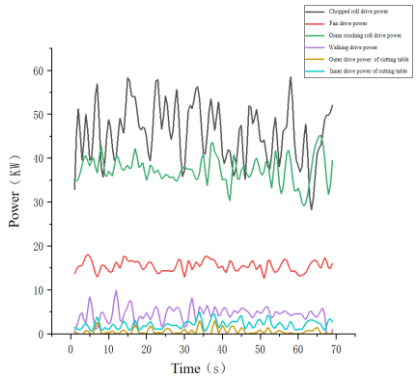

b) Average speed of 5.70 km/h, stubble height of 200 mm

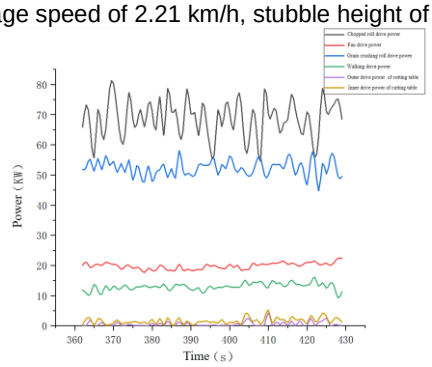

c) Average speed of 6.63 km/h, stubble height of 200 mm

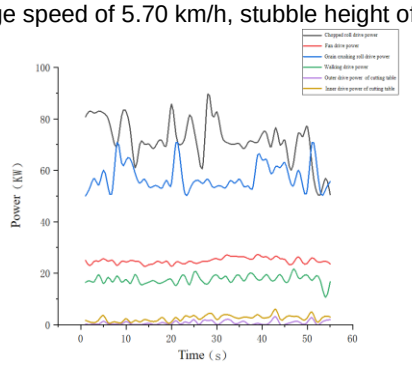

d) Average speed of 9.75 km/h, stubble height of 200 mm

Fig. 12 - Power curve of each key part

Table 4

Power distribution table of key parts

Test number	Engine Output/kW	Chopping roller drive power/kW	Fan drive power/kW	Grain crushing drive power/kW	Walking drive power/kW	Inside cutter drive power/kW	Outside cutter drive power/kW
1	154.19	37.54	10.04	20.31	10.41	3.07	0.57
2	208.17	55.76	15.42	37.33	20.80	3.38	0.66
3	263.63	68.70	19.87	47.30	26.12	3.62	0.61
4	271.75	76.05	23.06	57.29	30.01	3.74	0.73

Table 5

Standard deviation of power value of each key part

Test number	Engine Output/kW	Chopping roller drive power/kW	Fan drive power/kW	Grain crushing drive power/kW	Walking drive power/kW	Inside cutter drive power/kW	Outside cutter drive power/kW
1	5.363	12.14	0.234	9.53	3.35	1.024	1.357
2	6.766	14.61	0.371	11.67	3.71	2.93	2.038
3	7.397	15.25	0.41	11.38	1.37	1.31	1.827
4	13.505	22.65	0.52	17.12	5.41	1.494	1.173

Analyzing and comparing the above power data, it is learned that, 1) the inner and outer drive power of the cutting platform is small, and the value changes are not very big with the increase of the average speed and the feeding amount; the drive power of the chopping roller, the drive power of the fan, the drive power of the grain crushing roller, and the drive power of the walking are large, and the value changes are more obvious with the increase of the average speed and the feeding amount. 2) the average speed of the test 4 reaches 9.75 km/h, and the standard deviation of the power values of the key parts of the test prototype is large. At this time, the feeding volume is close to the limit value, and the standard deviation of the power value of each key part of the test prototype is large, indicating that the machine under the average speed, the power of each key part is unstable, and the long-time operation in this situation affects the life of the machine.

Further, the proportion of each key part to the engine output power under different working conditions and the relationship between them is analyzed. Figure 13 shows the power proportion of each key part.

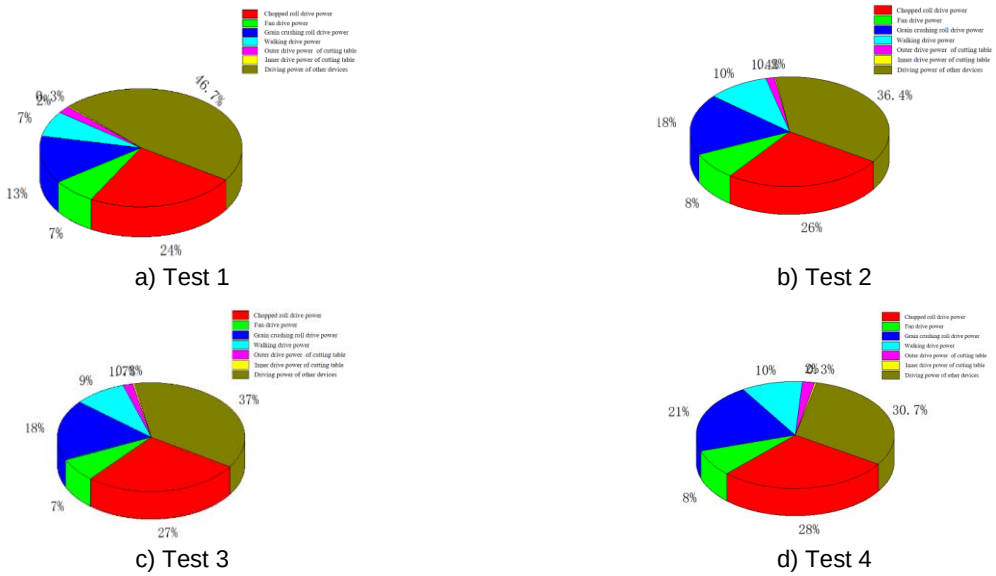

a) Test 1 b) Test 2

c) Test 3 d) Test 4

Fig. 13 - Power ratio chart of each key part

As can be seen in Figure 13: (1) the proportions of the inner and outer drive power of the cutting table, fan drive power and walking drive power to the engine output power are relatively stable, of which the proportion of fan drive power to the engine output power is 7% to 8%, and the proportion of walking drive power to the engine output power is 7% to 10%. Combined with Table 3-5 and Table 3-6, the standard deviation of the torque value of the fan drive shaft and walking drive shaft is small, and the load impact is relatively smooth. The inner and outer drive power of the cutting table accounts for 0.3% to 2% of the engine output power, which is small, but in the actual operation process, when the feeding volume is too large, it is easy to cause the cutting table blockage, in which case the load impact is larger. (2) The driving power of the chopping roller and the driving power of the grain crushing roller account for a large proportion of the engine output power, and the proportion of the range varies greatly. The proportion of chopping roller driving power is 24% to 28%, and the proportion of grain crushing roller driving power is 13% to 21%. When analyzing Table 4 and Table 5 together, Test 3 stands out as it ensures that the feed amount is close to the rated feed amount. Under this premise, the drive power for both the chopping roller and the grain crushing roller account for the smallest proportion of the engine's output power. Furthermore, the standard deviation of the torque value is smaller, indicating smoother fluctuations. Therefore, Test 3 represents the most ideal test conditions among the four groups of experiments.

CONCLUSIONS

This study realizes the torque and speed detection of the key components of the whole machine based on the strain bridge electrical measurement technology and CAN-bus communication technology, and the measurement parts cover most of the working parts of the test prototype. According to the structural characteristics of the working parts, wireless torque node, broken shaft method, strain gauges on the shaft method, extended shaft method, replacement pulley method and other methods are used to install torque sensors for the test prototype, and static calibration test and indoor bench loading test are carried out on the prototype of the torque sensors, which show that the torque sensors have a detection accuracy of 0.5%. This study can accumulate a large amount of field operation data of green fodder harvester under different working conditions, which can provide basic data support for the reasonable power allocation of each key working part of the whole machine and the analysis of the influence of the working power of each part on the operation quality of the machine. The results of the field test show that: the proportion of the inner and outer drive power of the cutting table, fan drive power and walking drive power of the green forage harvester to the engine output power are relatively stable, of which the proportion of the fan drive power to the engine output power is 7%-8%, the proportion of the walking drive power to the engine output power is 7%-10%, the proportion of the chopping roller drive power is 24%-28%, and the proportion of the driving power of grain crushing roller is 13%-28%, the proportion of the driving power of grain crushing roller is 13%-10%, and the proportion of the driving power of grain crushing roller is 13%-28%. When the speed is 6.63 km/h, under the premise of ensuring that the feeding amount is close to the rated feeding amount, the chopping roller driving power and the driving

power of grain crushing roller accounted for the smallest proportion of the engine output power, and the standard deviation of the torque value is small, and the fluctuation is relatively smooth, which is a more desirable test condition in the four groups of experiments.

ACKNOWLEDGEMENT

The work was sponsored by the Anhui Province science and technology major project (202203a06020027)

REFERENCES

[1] Buryanov A., Chervyakov I. (2019). Using combines for cleaning grain crops by non-traditional technologies, *INMATEH - Agricultural Engineering*. Vol. 59(3), pp. 27-32, DOI: http://doi.org/10.35633/INMATEH-59-03.

[2] Chen, M., Xu, G., Wei, M., Li, X., Wei, Y., Diao, P., Cui, P., Teng, S. (2023) Optimization design and experiment on feeding and chopping device of forage maize harvester. *International Journal of Agricultural and Biological Engineering*, Vol. 16(3), pp. 64-77, DOI: https://doi.org/10.25165/j.ijabe.20231603.7922.

[3] Cho, W., Lida, M., Suguri, M., Masuda, R., Kurita, H. (2014) Using multiple sensors to detect uncut crop edges for autonomous guidance systems of head-feeding combine harvesters. *Engineering in Agriculture, Environment and Food*, Vol. 7(3), pp.115-121, DOI: https://doi.org/10.1016/j.eaef.2014.02.004.

[4] Cho, J.B., Guinness, J., Kharel, T.P., et al. (2021) Spatial estimation methods for mapping corn forage and grain yield monitor data. *Precision Agriculture*, Vol. 22, pp. 1501-1520, DOI: https://doi.org/10.1007/s11119-021-09793-z.

[5] Feuerstein, U., Swieter, A. (2014). Evaluation effectiveness of forage harvesters in forage preparation. *IOP Conf. Ser.: Earth Environ. Sci.* 699, 012050, DOI: https://doi.org/10.1007/978-94-017-9044-4_18.

[6] Li, T., Li, N., Liu, C., Zhu, Z., Zhou, J., Zhang, H. (2021) Development of automatic depth control system employed in potato harvester (薯类收获机挖掘深度自动控制系统设计与试验). *Transactions of the Chinese Society of Agricultural Engineering*, Vol. 52(12), pp. 16-23, DOI: https://doi.org/10.6041/j.issn.1000-1298.2021.12.002.

[7] Liang, Z., & Wada, M. E. (2023). Development of cleaning systems for combine harvesters: A review. *Biosystems Engineering*, Vol. 236, pp. 79-102, DOI: https://doi.org/10.1016/j.biosystemseng.2023.10.018.

[8] Liu, L., Du, Y., Li, X., Liu, L., Mao, E., Guo, D., Zhang, Y. (2022) Trailer hopper automatic detection method for forage harvesting based improved U-Net. *Computers and Electronics in Agriculture*, Vol. 198, pp. 107046, DOI: https://doi.org/10.1016/j.compag.2022.107046.

[9] Liu, Y., Sun, D., Ni, X., Wang, S., Wang, Xin. (2022) Optimization of a Low Loss Strategy for Combine Harvesters Based on Bayesian Network. *IFAC-PapersOnLine*, Vol. 55(32), pp. 259-264, DOI: https://doi.org/10.1016/j.ifacol.2022.11.149.

[10] Mao, W., Han, S., Zhao, B. (2020). Study of remote monitoring system for forage harvester working condition based on Netty and Marshalling (基于 Netty 和 Marshalling 的青饲机工况远程监测系统研究). *Transactions of the Chinese Society of Agricultural Engineering*, Vol. 51, pp. 145-151, DOI: https://doi.org/10.6041/j.issn.1000-1298.2020.08.016.

[11] Martelli, R., Bentini, Ma., Monti, A. (2015) Harvest storage and handling of round and square bales of gian treed and switchgrass: an economic and technical evaluation. *Biomass Bioenergy*, Vol. 83, pp. 551-558, DOI: https://doi.org/10.1016/j.biombioe.2015.11.008.

[12] Mohsenimanesh, A., Nieuwenhof, P., Necsulescu, D. S., & Laguë, C. (2017). Monitoring a hydraulically-driven feed roll system with sensors on a prototype pull-type forage harvester. *Applied engineering in agriculture*, Vol. 33(1), pp. 23-30, DOI: https://doi.org/10.13031/aea.11645.

[13] Pallottino, F., Antonucci, F., Costa, C., Bisaglia, C., Figorilli, S., & Menesatti, P. (2019). Optoelectronic proximal sensing vehicle-mounted technologies in precision agriculture: A review. *Computers and Electronics in Agriculture*, Vol. 162, pp. 859-873, DOI: https://doi.org/10.1016/j.compag.2019.05.034.

[14] Siebald, H., Hensel, O., Beneke, F., Merbach, L., Walther, C., Kirchner, S. M., & Huster, J. (2017). Real-time acoustic monitoring of cutting blade sharpness in agricultural machinery. *IEEE/ASME Transactions on Mechatronics*, Vol. 22(6), pp. 2411-2419, DOI: https://doi.org/10.1109/TMECH.2017.2735542.

[15] Wang, F., Zhao, B., Liu, Y., Wang, J., Jiang, H. (2023). Design and Experiment of Multi-parameter Detection System for Corn Forage Harvester (玉米青贮收获机多参数检测系统设计与试验). *Transactions of the Chinese Society of Agricultural Engineering*. Vol.54(1), pp.127-136, DOI: https://doi.org/10.6041/j.issn.1000-1298.2023.01.013.

[16] Wang, J. (2019) *Development of metal foreign body detection system in harvesting machine*. Dissertation, Chinese Academy of Agricultural Mechanization Sciences, Beijing/China.

[17] Zhou, X., Xu, X., Zhang, J., Wang, L., Wang, D., Zhang, P. (2023) Fault diagnosis of forage harvester based on a modified random forest. *Information Processing in Agriculture*, Vol. 10(3), pp. 301-311, DOI: https://doi.org/10.1016/j.inpa.2022.02.005.

[18] Zhang, D., Yi, S., Zhang, J., Bao, Y. (2022) Establishment of millet threshing and separating model and optimization of harvester parameters. *Alexandria Engineering Journal*, Vol. 61(12), pp. 11251-11265, DOI: https://doi.org/10.1016/j.aej.2022.04.048.

[19] Wu, Z., Chen, J., Ma, Z., Li, Y., Zhu, Y. (2024) Development of a lightweight online detection system for impurity content and broken rate in rice for combine harvesters. *Computers and Electronics in Agriculture*, Vol. 218, pp. 108689, DOI: https://doi.org/10.1016/j.compag.2024.108689.

[20] Zhuohuai G., Zhou Z., Tao J., Ying L., Chongyou W., Senlin M. (2020). Development and test of speed control system for combine harvester threshing and cleaning device, *INMATEH – Agricultural Engineering*. Vol. 61 (2), pg. 305-314, DOI: https://doi.org/10.35633/inmateh-61-33